Control of N_2 fixation and NH_3 excretion in *Azorhizobium caulinodans* ORS571

Timothy L Haskett[a*], Ramakrishnan Karunakaran[b], Marcelo Bueno Batista [b], Ray Dixon[b] & Philip S Poole[a*].

[a]Department of Plant Sciences, University of Oxford, Oxford, OX1 3RB, UK.

[b]Department of Molecular Microbiology, John Innes Centre, Norwich, NR4 7UH, UK

*Corresponding author

Email tim.haskett@plants.ox.ac.uk

Abstract

Due to the costly energy demands of N_2 fixation, diazotrophic bacteria have evolved complex regulatory networks that permit expression of the N_2-fixing catalyst nitrogenase only under conditions of N starvation, whereas the same condition stimulates upregulation of high-affinity NH_3 assimilation by glutamine synthetase (GS), preventing excess release of excess NH_3 for plants. Diazotrophic bacteria can be engineered to excrete NH_3 by interference with GS, however control is required to minimise growth penalties and prevent unintended provision of NH_3 to non-target plants. Here, we attempted two strategies to control GS regulation and NH_3 excretion in our model cereal symbiont *Azorhizobium caulinodans Ac*LP, a derivative of ORS571. We first attempted to recapitulate previous work where mutation of both P_{II} homologues *glnB* and *glnK* stimulated GS shutdown but found that one of these genes was essential for growth. Secondly, we expressed unidirectional adenylyltransferases (uATs) in a Δ*glnE* mutant of *Ac*LP which permitted strong GS shutdown and excretion of NH_3 derived from N_2 fixation and completely alleviated negative feedback regulation on nitrogenase expression. We placed a *uAT* allele under control of the NifA-dependent promoter P*nifH*, permitting GS shutdown and NH_3 excretion specifically under microaerobic conditions, the same cue that initiates N_2 fixation, then deleted *nifA* and transferred a rhizopine-inducible $nifA_{L94Q/D95Q}$-*rpoN* controller plasmid into this strain, permitting coupled rhizopine-dependent activation of N_2 fixation with NH_3 excretion. In future, this highly sophisticated and multi-layered control circuitry could be used to activate N_2 fixation and NH_3 excretion specifically by *Ac*LP colonising transgenic rhizopine producing cereals, targeting delivery of fixed N to the crop, and preventing interaction with non-target plants.

Author Summary

Inoculation of cereal crops with associative "diazotrophic" bacteria that convert atmospheric N_2 to NH_3 could be used to sustainably improve delivery of nitrogen in agriculture. However, due to the costly energy demands of N_2 fixation, natural diazotrophic bacteria have evolved to conserve energy by preventing excess production of NH_3 and release to the plants. Diazotrophs can be engineered for excess NH_3 production and release, however genetic control is required to minimise growth penalties and prevent unintended provision of NH_3 to non-target weed species. Here, we engineer control of N_2 fixation and NH_3 excretion in response to the signalling molecule rhizopine which is produced by transgenic barley. This control could be used to establish plant host-specific activation of N_2 fixation and NH_3 release following root colonisation in the field, minimising bacterial energy requirements in the bulk soil and preventing provision of NH_3 to non-target plants.

Introduction

Nitrogen (N) is an essential constituent of all biological organisms, but metabolically accessible forms are scarce in most environments, restricting biomass production. In agriculture, productivity of cereal crops, which are a staple of human dietary requirements, requires large-scale supplementation with synthetic N fertilisers to meet global food security requirements (1). However, synthesis and excessive application of N fertilisers has a large energy cost, causes CO_2 release and results in loss of reduced N to the environment, which has doubled reactive N in the atmosphere and polluted waterways causing eutrophication and O_2-depleted dead zones (2). In contrast, N fertilisers are largely unaffordable to small-hold farmers in developing countries such as those in Sub-Saharan Africa (3), restricting yields to a fraction of their maximum potential (4). Inoculation of cereals with root-associative diazotrophic bacteria that convert atmospheric N_2 gas to NH_3 through the action of O_2-labile nitrogenase represents an affordable and sustainable alternative to the use of N fertilisers in agriculture (5-7). Although associative diazotrophs have been estimated to fix up to 70 kg N ha^{-1} $year^{-1}$ in agricultural systems (8), responses to inoculation are typically inconsistent due to sub-optimal competitiveness for root colonisation and persistence in soil (9-12). Furthermore, due to the costly energy demands of N_2 fixation, which consumes at least 16 mol ATP per mol N_2 fixed *in vitro*, bacteria have evolved complex regulatory networks that permit expression and activity of the N_2-fixing catalyst nitrogenase only under conditions of N starvation, whereas the same condition stimulates upregulation of high-affinity NH_3 assimilation by glutamine synthetase (*glnA*, GS), preventing excess release of excess NH_3 for plants (13, 14).

Associative diazotrophic bacteria can been engineered for excess production and excretion of NH_3 by several strategies (13, 15, 16). For example, in *Azotobacter vinelandii*, insertional inactivation of *nifL*, which encodes an O_2 as well as N and C sensing anti-activator of the nitrogenase master regulator NifA, drives constitutive nitrogenase activity resulting in excretion of NH_3 from the cell (17-20). The same effect was achieved by expressing mutant *nifA* alleles that are resistant to inhibition by NifL (18, 21, 22). While excess NH_3 production itself is likely to activate regulatory feedback mechanisms

reducing GS biosynthetic activity and NH_3 assimilation (15), mutating *glnA* (23-27) or genes involved in GS regulation may also be required to inhibit NH_3 assimilation more strongly and favour NH_3 excretion (28, 29).

Bacterial GS belongs to the "class I" type enzymes comprised of 12 identical subunits which are each adenylylated or de-adenylated by a bidirectional adenylyl transferase (AT, encoded by *glnE*) at the Tyr_{397} residue, with the fully de-adenylylated GS form being biosynthetically active and vice versa (30). Directionality of the ATase reaction is regulated by the post-translational modification state of P_{II} signal transduction proteins (31). The activity of P_{II} proteins is regulated by uridylylation/deuridylylation by the bidirectional uridylyltransferase (UT) GlnD which represents the most basal regulator in the cascade and can directly sense N status of the cell (32). GlnD uridylylates P_{II} under conditions of N-starvation and the resulting P_{II}-UMP ultimately triggers dephosphorylation of ATase and hence deadenylylation and activation of GS (33). In *Azorhizobium caulinodans* (*Ac*), insertional inactivation of both P_{II} homologues *glnB* and *glnK* produced a mutant that was unable to activate GS by deadenylylation, driving NH_3-insensitive N_2 fixation and excretion of NH_3 into the growth media (28). Critically, this engineering strategy does not appear to be universally applicable as P_{II} is essential for NifA and nitrogenase activity in some bacteria (34, 35), whereas it is essential for growth in others (36, 37). In a Δ*glnE* ATase mutant of *Azospirillum brasilense*, complementation with unidirectional adeyltransferase (uAT) alleles that encoded only the C-terminal adenylylation domain (31) drove strong adenylylation of GS resulting in excretion of NH_3 into the growth media (29). This strategy likely represents a more universally applicable approach for engineering NH_3 excretion in diazotrophs because the ATase is highly conserved, has a specific function, and can be readily mutated across diverse diazotrophic bacterial taxa (15, 38-40), albeit the mutation appears to be lethal in the heterotroph *Mycobacterium tuberculosis* (41, 42).

From an agricultural perspective, there are three major caveats of engineering diazotrophic bacteria for excessive production and excretion of NH_3; i) uncontrolled *nifA* and(or) nitrogenase expression has a severe energy burden on the cell that could abolish competitiveness for root colonisation; ii)

interference with GS activity typically renders strains auxotrophic for the essential amino acid glutamine, which could further reduce competitiveness; and iii) NH_3 excreting bacteria have potential to supply NH_3 to non-target weed species following promiscuous colonisation in the field. Therefore, establishing control of N_2 fixation and NH_3 excretion will be crucial for the optimisation of strains as agricultural inoculants. Control of NH_3 excretion has already been achieved in *A. vinelandii* by establishing IPTG-dependent expression of *glnA* (27), and in *A. brasilense* by establishing anhydro-tetracycline inducible expression of uATs (29, 43). However, use of plant-derived signals to control N_2-fixation and NH_3 excretion would be far more applicable in the environment and could impart partner-specificity to target delivery of fixed N to crops and prevent interactions with non-target host plants following promiscuous colonisation (44, 45).

We previously developed synthetic rhizopine signalling between barley and the model endophyte *Azorhizobium caulinodans Ac*LP that stimulates transcriptional activation of the mutant nitrogenase master regulator $nifA_{L94Q/D95Q,}$ which partially escapes nitrogen regulation, and when paired with the sigma factor RpoN drives N_2 fixation in bacteria colonising rhizopine producing (*RhiP*) barley roots (44, 46, 47). Here, we demonstrate that wild-type and engineered *Ac* strains do not release fixed N as NH_3 into the growth media when cultured under N_2-fixing conditions and therefore sought to engineer this trait by interfering with high-affinity NH_3 assimilation catalysed by GS. In our attempts to recapitulate NH_3 excreting *glnB glnK* double mutants of *Ac*LP (28), we found that deletion of both P_{II} homologues was only possible when second copy of *glnB* was first integrated into the chromosome suggesting one of the P_{II} homologues were essential for growth. GS and nitrogenase activity in the resulting strain exhibited minimal variation from that of the wild-type, but nevertheless the strain excreted low levels of NH_3 into the growth media. To optimise rates of NH_3 excretion, we utilised a second engineering strategy where a *Ac*LPΔ*glnE* mutant was complemented with uATs. In congruency with similar experiments performed in *A. brasilense* (29), uAT expression drove strong shutdown of GS, but also completely alleviated negative feedback inhibition of nitrogenase by NH_3 and stimulated NH_3 excretion. By placing uAT expression under control of NifA, we established control of these traits by the same cues that initiate N_2 fixation, then transferred rhizopine control of

129 *nifA*$_{L94Q/D95Q}$-*rpoN* into this strain linking activation of N_2-fixation and NH_3 excretion (Fig 1). This
130 highly sophisticated control circuitry represents a significant milestone in the development of a
131 "synthetic symbiosis" where N_2 fixation and NH_3 excretion could be activated in bacteria specifically
132 colonising target cereals, targeting delivery of N to the crops while avoiding potential interactions
133 with non-target plants.
134

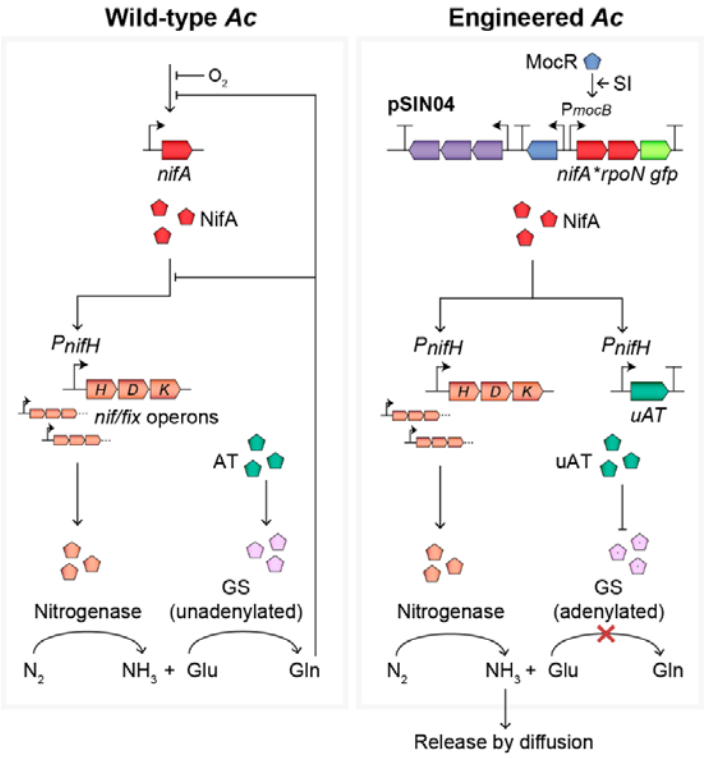

135
136

137 **Figure 1. Model for rhizopine control of N_2 fixation and NH_3 excretion in *Ac*.** In the wild-type
138 bacterium, NifA is activated under N_2-fixing (N-free microaerobic) conditions leading to transcription
139 of nitrogenase (*nif* and *fix*) genes and subsequently N_2 fixation. Under the same conditions, P_{II}-UMP
140 stimulates the adenylyltransferase (AT) to activate glutamine synthetase (GS) by deadenylylation. GS
141 catalyses assimilation of NH_3 via the conversion of glutamate (Glu) to glutamine (Gln), which feeds
142 back to repress *nif* expression and NifA activity, preventing excess production and release of NH_3
143 from the cell. In our engineered strain *Ac*PU-R22 carrying pSIN04, *nifA*$_{L94Q/F95Q}$ is expressed by

addition of rhizopine to the culture, driving nitrogenase expression and N_2 fixation. Additionally, NifA induces transcription of the unidirectional adenylyltransferase (uAT) which drives shutdown of GS by adenylylation, preventing NH_3 assimilation. Because shutdown of GS prevents glutamine biosynthesis, repression on *nif* gene expression and NifA activity is alleviated, resulting in excess production of NH_3 and release from the cell.

Results

Deletion or strong repression of the P_{II} genes is lethal

It was previously demonstrated that insertional inactivation of the *Ac* P_{II} genes *glnB* and *glnK* stimulates shutdown of GS by adenylylation and alleviates negative feedback inhibition of nitrogenase by the product NH_3, preventing NH_3 assimilation and favouring excretion into the growth media (28). We attempted to recapitulate these experiments in *Ac*LP, a derivative of *Ac* harbouring a mini-Tn7 *attB* integration site stably recombined into its chromosome, by constructing a markerless deletion of *glnB* and replacing *glnK* with an omega (Ω)-spectinomycin resistance (Sp) cassette. Although the single Δ*glnB* and Δ*glnK*::ΩSp mutations were readily acquired, we were unable to acquire the double mutant by introduction of the Δ*glnK*::ΩSp mutation into *Ac*LPΔ*glnB* when selection was performed on rich or minimal media supplemented with glutamine as a sole N source, suggesting the resulting phenotype was lethal. To explore this notion further, we integrated into the chromosome of *Ac*LPΔ*glnB* a construct encoding *glnB* with the strong ribosome binding site (RBS) RStd expressed from the IPTG de-repressible promoter P*lac* (Fig 2a) and were subsequently able to acquire the Δ*glnB* Δ*glnK*::ΩSp double mutation when selection was performed on rich media in the absence of IPTG, confirming that one of the P_{II} proteins was essential for growth.

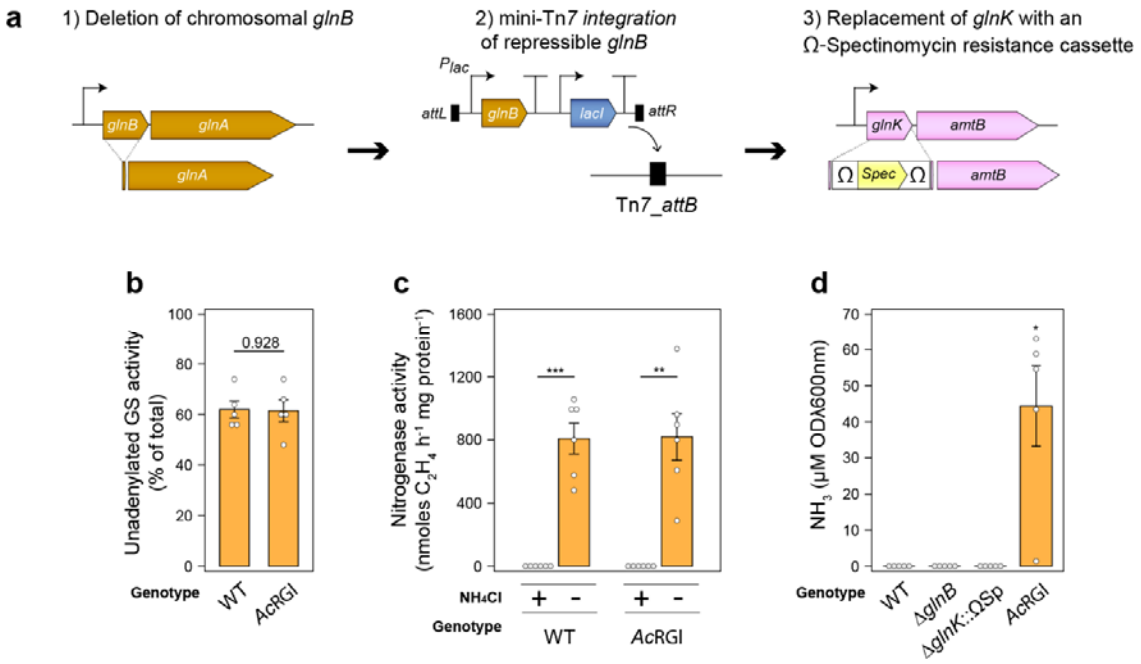

Figure 2. Strong repression of *glnB* in a *glnK* mutant has minimal effect on glutamine synthetase and nitrogenase activity but drives low-level NH_3 excretion. (a) Strategy for generating strain *Ac*RGl with the double Δ*glnB* and Δ*glnK*::ΩSp mutation following integration of an IPTG-derepressible *glnB* gene into the chromosome of *Ac*LP. **(b)** Activity of the unadenylylated (active) form of GS in $n = 5$ wild-type (WT) or *Ac*RGl cultures incubated for 24-h as determined by γ-glutamyl transferase assays in the presence or absence of 60 mM $MgCl_2$ (see S2 Fig for total activity). **(c)** Nitrogenase activity measured by acetylene reduction in $n = 6$ cultures between 3-h – 21-h **(d)** Spectrophotometric determination of NH_3 in media of $n = 5$ cultures grown for 24-h. Cultures for all assays were grown in N_2-fixing conditions (N-free UMS media with 3% O_2 in the headspace). Error bars represent one SEM. Independent two-tailed students t-tests were used to compare means. Exact P-values are provided where $P > 0.05$. *$P < 0.05$, **$P < 0.01$, ***$P < 0.001$. The wild-type *Ac*LP was used as a reference group for comparison of means in panel (e).

We next sought to test whether reduced translation of the introduced *glnB* module would stimulate GS shutdown and NH_3 excretion by tuning the ribosome binding site (RBS). Seven synthetic RBS' were experimentally demonstrated to produce translation rates spanning two to three orders of magnitude

(S1 Fig), but only when *glnB* fused to the strongest RBS "RStd" and integrated into the *Ac*LPΔ*glnB* chromosome were we able to subsequently isolate the Δ*glnK*::ΩSp mutation (hereby termed strain *Ac*RGl), suggesting that *glnB* had been repressed as much as was tolerable. We assessed total GS specific activity and that of the unadenylylated active enzyme in *Ac*RGl by performing γ-glutamyl transferase assays on whole cells in the presence or absence of 60 mM $MgCl_2$ which specifically inhibits the adenylylated enzyme (48), and found that mutant exhibited higher total GS activity compared to the wild-type (S2a Fig), presumably due to elevated *glnA* expression (S2b Fig) as is typical of *glnB* mutants (25, 28), whereas the adenylylation state of GS (depicted here as percentage of unadenylylated GS activity) was unchanged (Fig 2b). We also found that the specific nitrogenase activity of strain *Ac*RGl was no different from that of the wild-type, being repressed by supplementation of 10 mM NH_3Cl into the growth media (Fig 2c). Spectrophotometric quantification of NH_3 was next performed using the indophenol method (49) on the strains grown for 24-h under N_2-fixing conditions (here defined as N-free UMS with O_2 in the headspace adjusted to 3%). No NH_3 was detected in the wild-type or Δ*glnB* and Δ*glnK*::ΩSp single mutants, whereas we detected trace amounts of NH_3 in the growth media of strain *Ac*RGl (Fig 2d). Given that construction of the *Ac*LPΔ*glnB* Δ*glnK*::ΩSp double mutant was lethal, and strong repression of *glnB* had minimal effect on GS and nitrogenase regulation permitting only low-level NH_3 excretion, we concluded that these strategies were inadequate to establish control of NH_3 excretion in *Ac*LP and opted to pursue an alternative strategy.

uAT expression drives GS inactivation and NH_3 excretion

In a Δ*glnE* mutant of *A. brasilense*, controlled expression of a N-terminal truncated AT consisting of only the adenylylation domain results in unidirectional activity driving strong inactivation of GS by adenylylation and excretion of NH_3 into the growth media (29). We recapitulated these experiments in a Δ*glnE* mutant of *Ac*LP by using the *Sinorhizobium meliloti* derived P*nodA* promoter (S3 Fig), to drive expression of a series of truncated uATs derived from *Ac* or those previously described for *E. coli* (Fig 3a-b) (29). We assessed GS specific activity and that of the unadenylylated enzyme using γ-

213 glutamyl transferase assays on cells grown in N_2-fixing conditions for 3-h and confirmed that leaky
214 non-induced uAT expression stimulated GS adenylylation (Fig 3c), while having minimal effect on
215 total GS specific activity relative to wild-type bacteria (S4 Fig). The strains also excreted between
216 0.1-1.5mM of NH_3 after 24-h incubation in N_2-fixing conditions, whereas the wild-type and Δ*glnE*
217 mutant did not excrete detectable levels of NH_3 (Fig 3d). Interestingly, we found that NH_3 excretion
218 was sub-optimal when the P*nodA* promoter controlling *uAT* expression was induced with saturating
219 levels (5 uM) of naringenin (S5 Fig), suggesting that *uAT* overexpression is metabolically detrimental,
220 as was observed in *A. brasilense* (43). This indicated that more finely tuned *uAT* expression would be
221 critical to achieve stringent control of GS adenylylation in *Ac*LP.
222

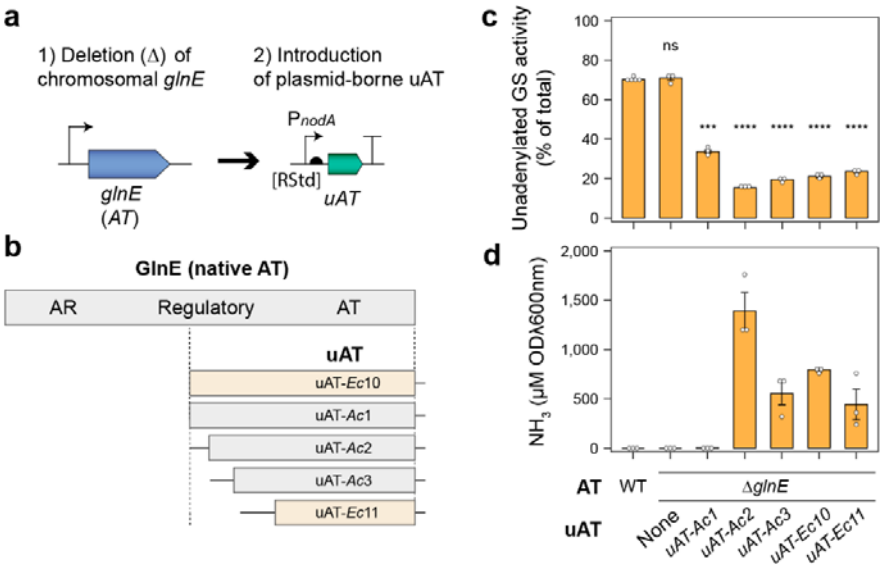

223

224 **Figure 3. uAT expression drives GS adenylylation and NH_3 excretion in a Δ*glnE* background. (a)**
225 Strategy for complementation of the Δ*glnE* mutation with naringenin-inducible unidirectional
226 adenylyltransferases (uAT) expressed from low-copy parent plasmid pOPS1536. **(b)** A series of
227 truncated uAT proteins were used in this study. The *uAT-Ec10* and *uAT-Ec11* alleles are derived from
228 *E. coli* were described previously (29), whereas *uAT-Ac* alleles are derived from *Ac*LP. The nucleotide
229 sequences for these alleles are provided in S1 File. **(c)** Activity of the unadenylylated (active) form of
230 GS in $n = 5$ for *Ac*LP (wild-type, WT) or $n = 3$ cultures incubated for 3-h in N_2-fixing conditions (N-
231 free UMS media with 3% O_2 in the headspace) without the inducer naringenin as determined by γ-

glutamyl transferase assays in the presence or absence of 60 mM $MgCl_2$ (see S4 Fig for total activity). **(d)** Spectrophotometric determination of NH_3 in media of n = 3 cultures grown for 24-h in N_2-fixing conditions. Error bars represent one SEM. Independent two-tailed students t-tests with the Bonferroni-holm adjustment were used to compare means using the wild-type *Ac*LP as a reference group. Not significant (ns P > 0.05), ***P < 0.001, ****P < 0.0001.

Shutdown of glutamine biosynthesis alleviates negative feedback on nitrogenase

Expression of *uAT* restricts glutamine production via the high affinity GS-dependent NH_3 assimilation pathway, providing us with a unique opportunity to tease apart the effects of NH_3 and glutamine on the nitrogenase (*nif*) gene expression. We postulated that NH_3 must first be converted into glutamine to mediate repression of *nif* genes and tested this hypothesis first by examining expression of P*nifH* fused to *GFP* on plasmid pOPS1213 in wild-type bacteria and in *Ac*LPΔ*glnE* expressing the *uAT-Ac2* allele from the non-induced P*nodA* promoter on a second plasmid. As expected, P*nifH*::*GFP* activity in both strains grown under microaerobic conditions (3% O_2 in the headspace) was strongly repressed by supplementation with 10 mM glutamine however, while P*nifH*::*GFP* was repressed in the wild-type by supplementation with 10 mM NH_4Cl, P*nifH*::*GFP* expression was not repressed by NH_4Cl in *Ac*LPΔ*glnE* expressing *uAT-Ac2* (Fig 4a). We observed a similar pattern when nitrogenase activity was assessed by ARAs (Fig 4b-c), indicating that NH_3 itself has no effect on negative feedback regulation of *nif* genes but must be converted into glutamine or potentially other amino acids to facilitate repression. Engineering NH_3 excreting bacteria by targeted GS shutdown therefore has two advantages; i) alleviating negative feedback regulation of *nif* genes and ii) preventing NH_3 assimilation to favour release.

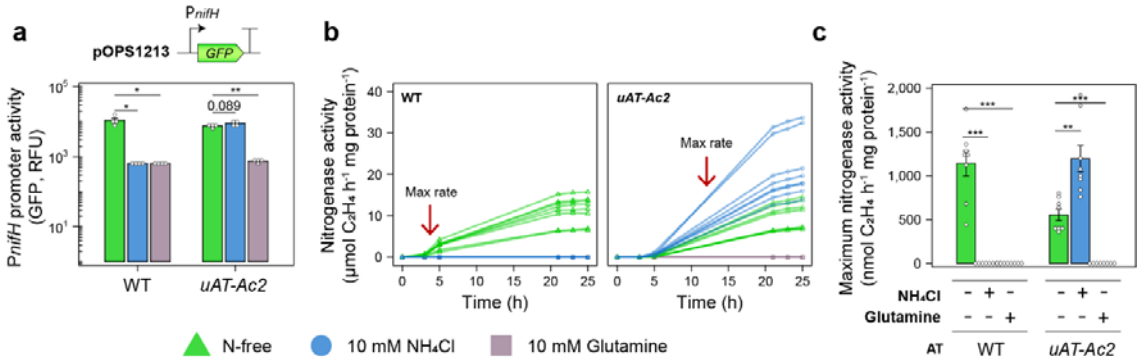

Figure 4. uAT expression abolishes negative feedback regulation on nitrogenase. (a) A P*nifH*::*GFP* reporter carried on plasmid pOPS1213 was mobilised into the wild-type (WT) *Ac*LP and *Ac*LPΔ*glnE* expressing *uAT-Ac2* on a second low-copy plasmid and induction was measured in $n = 4$ cultures grown for 24-h under the conditions indicated. Relative fluorescence units (RFU) are defined here as GFP fluorescence / OD600λnm **(b)** Nitrogenase activity was measured by acetylene reduction in $n = 8$ cultures grown under N_2-fixing conditions (N-free UMS media with 3% O_2 in the headspace) and **(c)** the maximum rates are presented. Error bars represent one SEM. Independent two-tailed students t-tests with Bonferroni-holm adjustment were used to compare means. Exact P-values are provided where P > 0.05. **P < 0.01, ***P < 0.001. WT bacteria grown at 3% O_2 in N-free conditions was used as a reference group for statistical comparisons in panel (a).

NifA control of *uAT* expression

As a direct consequence of engineering NH_3 excretion through GS interference, bacteria typically become auxotrophic for glutamine. While this may not be non-problematic for cultures grown *in vitro* under gnotobiotic conditions, glutamine auxotrophs in the field would be unable to compete or persist in the soil and rhizosphere. In rhizobia-legume symbioses, rhizobia only restrict NH_3 assimilation after infecting the low-oxygen environment of the nodule and differentiating into an N_2 fixing bacteroid (50, 51), allowing them to maintain competitiveness during their free-living state in the soil. To mimic this regulation, we fused the *uAT-Ac2* allele to native or synthetic RBSs and placed these

279 under control of the NifA-inducible P*nifH* promoter on mini-Tn*7* delivery plasmids, then integrated
280 these into the chromosome of *Ac*LPΔ*glnE*, creating strains *Ac*PU-RStd, *Ac*PU-R1, *Ac*PU-R22, *Ac*PU-
281 R31, *Ac*PU-Rnat and *Ac*PU-R28 (Fig 5a). When grown under aerobic (21% O_2) conditions in the
282 presence of 10 mM NH_4Cl, growth of *Ac*LPΔ*glnE* expressing the *uAT-Ac2* allele from the non-
283 induced P*nodA* promoter was almost entirely abolished compared to where glutamine was provided as
284 a source of N (Fig 5b and S6 Fig). In contrast, the growth characteristics of strains expressing *uAT-*
285 *Ac2* from the P*nifH* promoter were reminiscent of the wild-type *Ac*, except for strains where *uAT-Ac2*
286 was fused to the strongest RBS' RStd or R1, which increased mean generation times (MGT) but did
287 not affect the total biomass at stationary phase (Fig 5b and S6 Fig). We next assessed GS regulation
288 by γ-glutamyltransferase assays and confirmed that under aerobic conditions in the presence of 10
289 mM NH_4Cl, the percentage of active deadenylylated GS activity in strains *Ac*PU-R1, *Ac*PU-R22, and
290 *Ac*PU-R3 closely resembled that of the wild-type, suggesting that NH_3 assimilation was functional.
291 When grown under microaerobic conditions (3% O_2) in the presence or absence of 10 mM NH_4Cl, GS
292 in wild-type *Ac*LP was activated by de-adenylylation, whereas GS in all *Ac*LPΔ*glnE* strains
293 expressing uAT-*Ac*2 from the P*nifH* promoter became more heavily inactivated by adenylylation
294 under the same conditions (Fig 5c), with the percentage unadenylated GS activity correlating
295 negatively with the strength of RBS fused to *uAT-Ac2*. We finally performed NH_3 excretion assays on
296 the engineered strains and found that each excreted NH_3 into the growth media after 24-h, except for
297 where *uAT-Ac2* was fused to the weakest RBS [R28] (Fig 5d). Overall, the data suggested that by
298 expressing *uATs* from the P*nifH* promoter, GS shutdown can be controlled in response to the same
299 cues that initiates N_2 fixation.
300
301

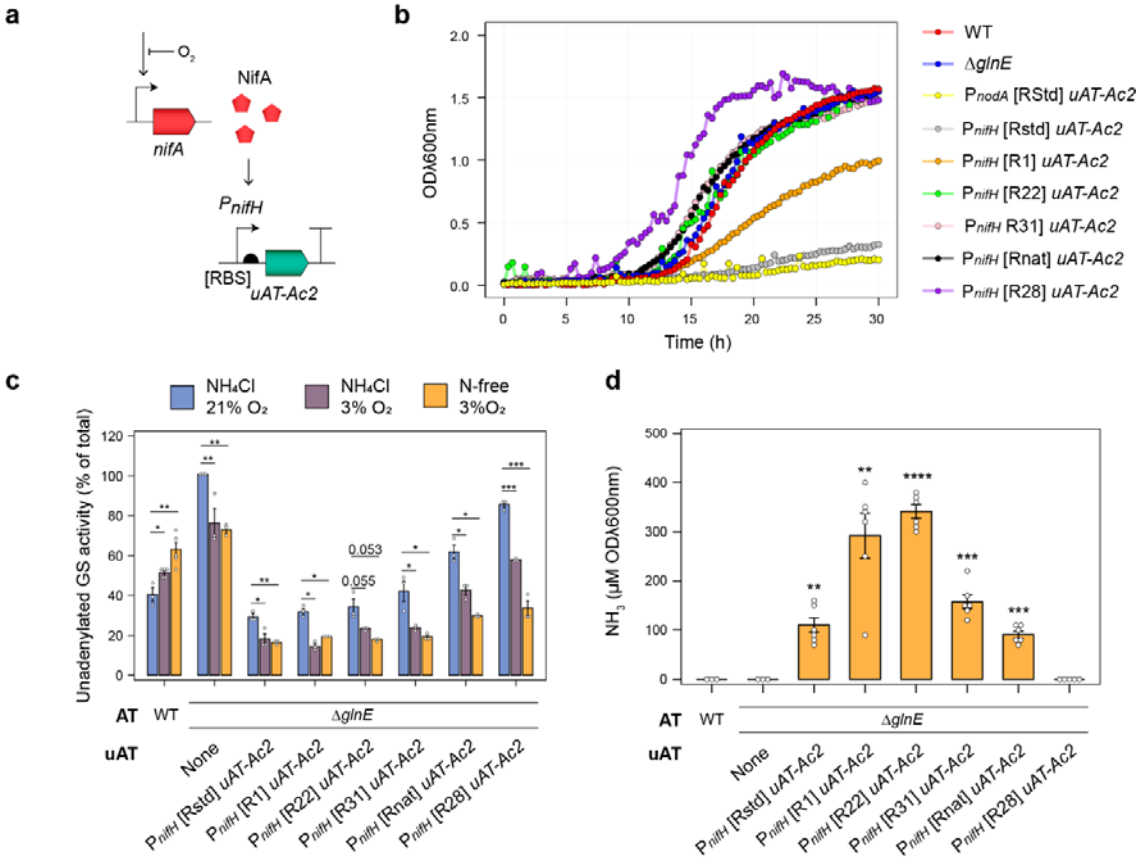

Figure 5. Coupled activation of N_2 fixation and GS adenylylation via NifA-dependent expression of *uAT*. **(a)** Strategy for complementation of the Δ*glnE* mutation with NifA-inducible unidirectional adenylyltransferases (uAT) integrated into the chromosome using mini-Tn*7*. **(b)** Growth of control strains and those expressing uATs in UMS media supplemented with 20 mM succinate and either 10 mM glutamine or 10 mM NH_3Cl under aerobic conditions. See S6 Fig for full growth statistics. **(c)** Activity of the unadenylylated (active) form of GS in n = 5 for wild-type (WT) *Ac*LP or n = 3 cultures incubated for 24-h in as determined by γ-glutamyl transferase assays in the presence or absence of 60 mM $MgCl_2$. (**d**) Spectrophotometric determination of NH_3 in media of n = 3 WT and Δ*glnE* or n = 5 cultures grown for 24-h in N_2-fixing conditions (N-free UMS media with 3% O_2 in the headspace). Error bars represent one SEM. Independent two-tailed students t-tests with the Bonferroni-holm adjustment were used to compare means using the wild-type *Ac*LP as a reference group. Exact P-values are provided where P > 0.05. **P < 0.01, ***P < 0.001. WT bacteria were used as a reference group for statistical comparisons in panels (a) and (b).

Rhizopine-dependent control of N_2 fixation, GS adenylylation and NH_3 excretion

While NifA-dependent expression of nitrogenase and *uAT-Ac2* in *Ac*Δ*glnE* drives N_2 fixation and GS inactivation leading to NH_3 excretion, the lack of plant host-specific signalling to drive these processes could permit bacteria to supply NH_3 to target crops and non-target weed species alike. We previously used synthetic rhizopine signalling to establish control of a mutant *nifA* allele (encoding $NifA_{L94Q/D95Q}$) and *rpoN* in *Ac*LPΔ*nifA* carrying plasmid pSIN02, which drove partially NH_3-resistant activation of nitrogenase activity specifically by bacteria occupying the roots of transgenic *RhiP* barley (46). We performed NH_3 excretion assays on *Ac*LPΔ*nifA* carrying pSIN02 and found that this strain did not secrete NH_3 into the growth media (S7 Fig). Thus, we opted to establish rhizopine control of the *nifA*$_{L94Q/D95Q}$-*rpoN* operon in our strain *Ac*PU-R22 where *uAT-Ac2* expression placed under control by NifA. We first tested in *Ac*LP, induction of a new rhizopine receiver plasmid pSIR03 which was derived from the high-copy rhizopine receiver pSIR03 but carried an RK2 replicon for low-copy maintenance. Using *GFP* induction assays, we demonstrated that pSIR03 (Fig 6a) has a dynamic range of 162-fold in response to the rhizopine *scyllo*-inosamine (SI) and was induced in 93.08 ± [SEM] 0.32% of cells in populations when 10 µM SI was supplemented *in vitro* (Fig 6b-c & Table S1). We deleted the native *nifA* gene from strain *Ac*PU-R22 and introduced a rhizopine *nifA*$_{L94Q/D95Q}$-*rpoN* controller plasmid pSIN04 which was derived from pSIR03 (Fig 6d). Expression of *nifA*$_{L94Q/D95Q}$-*rpoN* under microaerobic conditions by addition of 10 µM SI into the media resulted in tightly controlled activation of nitrogenase that was unimpeded by addition of 10 mM of NH_3 (Fig 6e). Moreover, GS was strongly adenylylated by addition of 10 SI to the media in both aerobic and microaerobic conditions (Fig 6f). Because NifA in many diazotrophs is inactivated when cells are grown at 21% O_2 (52), we subsequently tested O_2 tolerance of our $NifA_{L94/D95Q}$ mutant protein by inducing expression of *nifA*$_{L94Q/D95Q}$-*rpoN* in *Ac*LPΔ*nifA* carrying pSIN03 with rhizopine and monitoring activation of the P*nifH::GFP* promoter fusion (S8a Fig). Interestingly, the $NifA_{L94/D95Q}$ protein activated P*nifH::GFP* 13-fold ± [SEM] 1.5 and 98-fold ± [SEM] 2.8 under aerobic and microaerobic conditions, respectively (S8b Fig), suggesting that the protein is tolerant to oxygen.

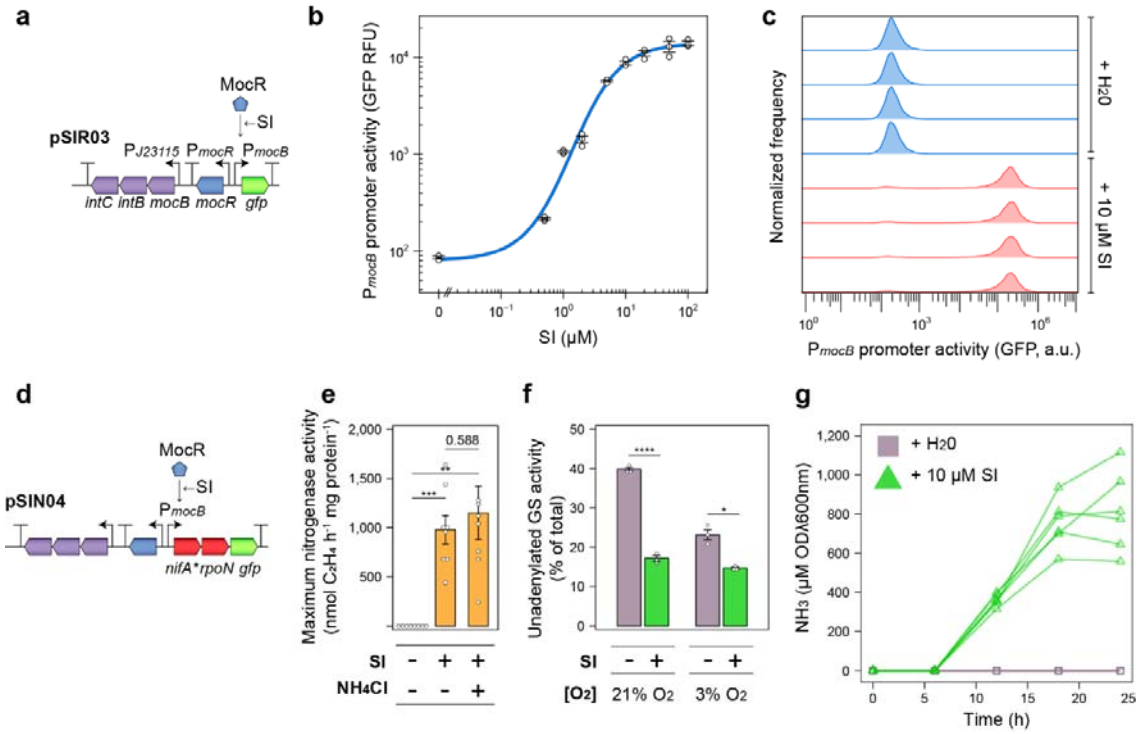

Figure 6. Rhizopine control of N_2 fixation, GS adenylylation and NH_3 excretion. (a) Genetic schematic (not to scale) of the low-copy (RK2 replicon) rhizopine receiver plasmid pSIR03. **(b)** Dose response of GFP induction in *Ac*LP (*n* = 3) harbouring pSIR03 with the rhizopine *scyllo*-inosamine (SI) supplemented *in vitro*. Relative fluorescence units (RFU) are defined here as GFP fluorescence / OD600λnm. **(c)** Flow-cytometry analysis of GFP fluorescence in *Ac*LP (*n* =4) harbouring pSIR03 incubated for 24-h in the absence or presence of 10 μM rhizopine. See Table S1 for full statistics. **(d)** Genetic schematic (not to scale) of the low-copy (RK2 replicon) rhizopine $nifA_{L94Q/D95Q}$-*rpoN* controller plasmid pSIN04. **(e)** Optimal nitrogenase activity of *Ac*PU-R22 Δ*nifA* carrying pSIN04 measured between 5-h – 21-h by acetylene reduction in *n* = 6 cultures grown under microaerobic conditions (3% O_2 in the headspace). **(f)** Activity of the unadenylylated (active) form of GS in *n* = 3 cultures of *Ac*PU-R22 Δ*nifA* carrying pSIN04 incubated for 24-h as determined by γ-glutamyl transferase assays in the presence or absence of 60 mM $MgCl_2$. **(g)** Spectrophotometric determination of NH_3 in media of *n* = 6 cultures of *Ac*PU-R22Δ*nifA* carrying pSIN04 grown in N_2-fixing conditions (N-free UMS media with 3% O_2 in the headspace) in the presence of absence of 10 μM SI. Error bars represent one SEM. Independent two-tailed students t-tests with the Bonferroni-holm adjustment were

used to compare means. Exact P-values are provided where P > 0.5. **P < 0.01, ***P < 0.001, ****P < 0.0001.

We finally performed NH_3 excretion assays on cultures of strain *Ac*PU-R22 carrying pSIN04 supplemented with 10 μM SI and demonstrated that the strain excreted 812.58 ± [SEM] 5.59 uM ODλ600nm^{-1} NH_3 into the growth media after 24-h incubation in N_2-fixing conditions at an optimal rate of 65.13 ± 7.35 uM OD600nm^{-1} h^{-1} (Fig 5g). Importantly, no NH_3 excretion was detected in the absence of SI, demonstrating tight control. Overall, these experiments confirmed that we had established rhizopine control of N_2-fixation, GS adenylylation and NH_3 excretion in our engineered *Ac*LP strain.

Discussion

In this study, we employed two strategies to interfere with GS and stimulate NH_3 excretion in *Ac*LP. For our first strategy, we attempted to recapitulate previous experiments where insertional inactivation of the P_{II} genes *glnB* and *glnK* stimulated shutdown of GS by adenylylation and alleviated negative feedback inhibition of nitrogenase by the product NH_3, preventing NH_3 assimilation and favouring excretion into the growth media (28). Although we could delete either of the *glnB* or *glnK* genes from *Ac*LP, we were unable to delete both genes in the same strain unless a second copy of *glnB* was first introduced into the chromosome, suggesting at least one of the P_{II} coding sequences was essential for growth. Considering that a P*aph*::KIXX kanamycin resistance cassette was previously inserted to the 3'-end of the *Ac glnB* coding sequence (25) leaving most of the 5'-end reading frame intact, it seems possible that the GlnB protein may have retained some essential function unrelated to AT and GS activity. In contrast, previous insertion of the omega interposon into *Ac glnK* replaced a segment of the internal coding sequence and was therefore more likely to have abolished the function of the protein (53). Interestingly, similar *glnB* and *glnK* antibiotic cassette insertions have been made in the phototrophic diazotroph *Rhodobacter capsulatus*, resulting in NH_3-insensitive NifA and nitrogenase

387 expression and activity (54). However, attempts to delete both genes were also unsuccessful in this
388 bacterium (55). Regardless of why deleting *glnB* and *glnK* is lethal, reproducing exact copies of the
389 original *glnB* and *glnK* mutants (28) would likely be required to establish control of NH_3 excretion in
390 *Ac*LP, as we have shown here that deletion of *glnK* paired with strong repression of *glnB* had minimal
391 effect on nitrogenase or GS regulation and permitted only low-level NH_3 excretion.
392
393 As was previously demonstrated in *A. brasilense* (29), expression of *E. coli* or *Ac*-derived uATs in our
394 *Ac*LPΔ*glnE* mutant resulted in strong GS shutdown and high rates of NH_3 excretion when grown in
395 N_2-fixing conditions. We also found that while nitrogenase expression and activity is repressed in
396 microaerobic NH_3 or glutamine-fed cultures of *Ac*LP, shutdown of glutamine biosynthesis by uAT
397 expression resulted in nitrogenase expression that was unimpeded by NH_3 but still repressed by
398 glutamine, suggesting that NH_3 must first be converted to glutamine or potentially other amino acids
399 such as asparagine (56) to facilitate repression. This same effect was previously reported in
400 phototrophic *Anabaena* spp (57, 58) and *Rhodobacter sphaeroides* (59) where GS activity was
401 shutdown using the chemical inhibitor L-Methionine sulfoximine, and in *Klebisella pneumoniae*
402 mutants unable to grow on NH_3 as a sole source of N (60). Moreover, In *R. capsulatus*, where N_2-
403 fixation is repressed in response to added NH_3 at three levels; a) NtrC-dependent transcription of *nifA*;
404 b) NifA-dependent transcription of nitrogenase; and c) DraT-DraG-dependent ADP ribosylation of
405 nitrogenase (61, 62); all three levels of regulation were non-responsive to NH_3 following shutdown of
406 GS by insertional inactivation of both P_{II} genes (54). Thus, it seems plausible that shutdown of
407 glutamine biosynthesis from NH_3 and glutamate abolishes NH_3-dependent regulation of N_2-fixation in
408 genetically diverse bacteria. Targeted GS shutdown therefore affects NH_3 excretion on two fronts,
409 allowing sustained nitrogenase expression and activity in the presence of fixed N_2 and preventing
410 assimilation of NH_3, favouring excretion into the environment.
411
412 Without establishing control of GS shutdown, engineered NH_3 excreting diazotrophs are typically
413 auxotrophic for glutamine, which would render them non-competitive in the environment (13, 16).
414 Here, we placed expression of the *uAT-Ac2* allele under control of the NifA-inducible nitrogenase

415 promoter P*nifH* which, when tuned correctly, triggered GS shutdown and NH_3 excretion specifically
416 under N_2-fixing conditions. In the field, this could allow bacteria to retain competitiveness prior to
417 forming O_2-deplete biofilms on the surface of roots (63), however lack of host-specific control could
418 permit provision of NH_3 to non-target plant species. Thus, we further modified the engineered strain
419 *Ac*PU-R22 by deleting *nifA* and bringing the mutant $nifA_{L94Q/D95Q}$ and *rpoN* alleles under rhizopine-
420 inducible control, permitting *in vitro* rhizopine-dependent activation of nitrogenase activity, GS
421 shutdown and NH_3 excretion. The resulting strain should also only activate these processes when
422 colonising the roots or rhizosphere of transgenic *RhiP* barley (47), though we acknowledge that
423 experimental demonstration of this will first require optimisation of the current rhizopine signalling
424 circuitry that permits perception of rhizopine by 10-25% of cells colonising *RhiP* barley roots and
425 activation of nitrogenase activity equating to approximately 15% of that observed for wild-type *Ac*LP
426 cells colonising wild-type barley (46). We have made progress on improving rhizopine signalling here
427 as our new low-copy rhizopine receiver plasmid pSIR03 permitted rhizopine-responsive GFP
428 activation in over 90% of cells in the population, compared to our previously reported plasmid
429 pSIN02 where only 36% of cells perceived rhizopine *in vitro* (46). Moving forward, increasing the
430 proportion of *Ac* cells sensing rhizopine on the root surface and rhizosphere will be crucial to
431 establish effective control of traits.
432
433 With bacteria engaging in partner-specific activation of NH_3 excretion, there still exists the possibility
434 that viability and competitiveness might suffer due to increased energy demand (14). Rhizobia
435 overcome this problem by engaging in stringent signalling with the legume that permits partner-
436 specific infection of nodules (64). Inside the nodule, the bacteria are provided with low-oxygen
437 conditions conducive to nitrogenase stability, they can escape the fierce competition of the
438 rhizosphere, and are fed carbon in the form of dicarboxylates (50, 51). Engineering a nodule-like
439 niche with stringent entry requirements into cereals will likely be important to maximise the
440 effectiveness of inoculation with engineered NH_3 excreting inoculants. The strains developed here
441 could be adapted for entry of such an environment and therefore, this work represents significant
442 advancement towards the development of both associative and more intimate "synthetic N_2-fixing

443 symbiosis" with cereals.

444

445 Materials and methods

446 Bacterial strains and plasmids

447 Bacteria used in this study (S1 File) were cultured in TY (65) or UMS (66, 67) media supplemented
448 with 300 μM nicotinic acid and 20 mM succinate as previously described (46). Plasmids (S2 Table)
449 were constructed using HiFi assembly (New England Biolabs) or BEVA modular golden-gate
450 assembly (68, 69) as outlined in the S1 File and were mobilised into *Azorhizobium* by diparental
451 mating with *E. coli* ST18 (70). For mini-Tn*7* integration into the chromosome, tri-parental matings
452 were used to additionally mobilise the transposase helper plasmid pTNS3, which carries an R6K
453 origin of replication that is not maintained in *Azorhizobium* (71).

454

455 Gene deletion and replacement mutant strains were constructed by mobilising the relevant suicide
456 plasmid, derived from pK19mobSacB (S2 Table & S1 File), into the target strain and selecting for
457 single-crossover integration into the chromosomal region of interest by plating cells on selective UMS
458 or TY agar media supplemented with 100 μg mL^{-1} kanamycin. Single-crossover mutants were
459 subsequently grown in non-selective media until stationary phase and plated in serial dilutions onto
460 UMS or TY agar supplemented with 10% (v/v) sucrose to select for double crossover deletion or
461 replacement of the target gene. For the *ΔglnK*::Ω*Sp* replacement plasmid pOPS1564 only, 100 μg mL^{-1}
462 spectinomycin and 1 mM IPTG was added to the media unless otherwise stated. Single colonies
463 were patched onto the same media used for double-crossover selection plus and minus 100 μg mL^{-1}
464 kanamycin and kanamycin sensitive colonies were screened by PCR and sanger sequencing for
465 deletion or replacement of the target gene.

466

467 All *Ac*LP *ΔglnB ΔglnK*::Ω*Sp* mutant strains were constructed by first deleting *glnB* from *Ac*LP using
468 plasmid pOPS1691, then subsequently integrating the *ΔglnK*::Ω*Sp* replacement plasmid pOPS1564

into the target chromosomal region by single-crossover. Because replacement of *ΔglnK*::Ω*Sp* was not possible on three separate occasions, mini-Tn*7* delivery plasmids carrying an IPTG-derepressible copy of *glnB* (S1 File) were integrated into the engineered *attB* site prior to selecting for selecting for double-crossover replacement of *glnK* with the Ω*Sp* interposon as described above.

Growth curves

Growth curves were performed in triplicate by streaking single colonies onto 10 mL TY agar slopes and incubating for 3-days prior to three washes in PBS and inoculation at OD600λnm 0.01 into 500 µL UMS media in 24-well plates. The OD600λnm was monitored at 20 min intervals in an Omega FLUOstar plate reader set to shake cultures at 700 rpm at 37 °C until stationary phase. Growth statistics were calculated using the R package GrowthCurver (72).

Glutamine synthetase transferase assays

Six-millilitre UMS cultures were initially grown in 30 mL glass universal vials sealed with silicone rubber septa as described for RT-qPCR experiments. After 3-h or 24-h incubation, 1 mL of culture was sampled for protein determination using a Millipore BCA protein assay kit. Five hundred microlitres of CTAB (1 mg mL^{-1}) was added to the remaining cultures which were incubated at room temperature for a further 3 mins prior to harvesting by centrifugation at 4 °C. Cells were washed once with 5 mL 1% (w/v) KCL and finally resuspended in 500 µL of the same buffer and stored on ice. GS transferase assays were performed on 50 µL aliquots the permeabilised cells as previously described (15). The assays were performed in 500 µL total volumes with 30 min incubation in the presence or absence of 60 µM added Mg^{2+} to determine the total GS transferase activity and the activity of the "active" unadenylylated enzyme, respectively (48). The GS transferase buffer was adjusted to pH 7.0, as this was previously estimated as the iso-activity point for *Ac* (73). Following addition of the $FeCl_3$ stop reagent, reaction tubes were centrifuged for 5 min at 13,000 g and 200 µL was transferred to clear, flat bottomed 96-well plates for spectrophotometric quantification of the product L-Glutamyl-γ-Hydroxamate (LGH) at 562λnm in a Promega GloMax multi-detection system.

Acetylene reduction assays

Cultures for ARAs were prepared and analysed as previously described (46, 74) and 1 mL samples of the headspace atmosphere were analysed using a PerkinElmer Clarus 480 gas chromatograph equipped with a HayeSep® N (80–100 MESH) 584 column at 3-h, 5-h, 21-h, 23-h and 25-h incubation, unless otherwise stated.

NH_3 excretion assays

Three-millilitre UMS cultures were initially grown in 30 mL glass universal vials sealed with silicone rubber septa as described for RT-qPCR experiments. OD600λnm was recorded and NH_3 was quantified in spent supernatants using the spectrophotometric indophenol assay as previously described (15). A calibration curve was performed for each experiment using freshly made dilutions of NH_3Cl in UMS ranging from 5 µM – 1 mM. Absorbance of indophenol blue was quantified in a Genesys 150 UV visible spectrophotometer (Thermo Scientific) at 652λnm after 4-h incubation at room temperature.

RT-qPCR

For RT-qPCR experiments, n=5 single colonies were streaked onto 10 mL UMS agar slopes supplemented with 20 mM succinate, 10 mM NH_4Cl and 300 µM nicotinate and grown for 2-days at 37 °C. Cells were washed three times from the slopes with PBS, resuspended in UMS supplemented with the relevant carbon and N sources at OD600λnm 0.3 in 30 mL glass universal vials and transferred with the lid off into a sealed atmosphere cabinet adjusted to 3% O_2 by flushing with N_2 gas. After 30 min, cultures were sealed with silicone rubber septa and incubated at 37 °C with rigorous shaking for 3-h. Cells were next harvested by centrifugation at 4 °C, lysed using a FastPrep-24 5G instrument and cellular debris was removed by a second round of centrifugation. RNA was extracted from the resulting lysate using a Qiagen RNAeasy extraction kit and tested for quality and

purity using an Agilent Experion Bioanalyzer with RNA Stdsens chips. gDNA was depleted from RNA by treatment with Invitrogen Turbo DNAse as per the manufacturer's recommendations and 5 µg was used to generate cDNA using an Invitrogen SuperScript IV reverse transcriptase kit as per the manufacturer's recommendations. The final cDNA template was diluted 1:20 with water and 1 µL was added to each 20 µL RT-qPCR reaction prepared in 96-well plates with Applied Biosystems PowerUp SYBR green master mix. Reactions were run using an Applied Biosystems ViiA 7 Real-Time PCR system. RT-qPCR primers were initially tested for amplification efficiency and target specificity by generating a standard curve of amplification with 5-fold dilutions of *Ac*LP gDNA. The housekeeping gene primer targeted *recA* and was validated previously (75), whereas the *glnA* primers designed here had the following sequence *glnA F* 5'- CCGCTGACCAACTCCTACA *glnA R* 5'-CCATGAACAGGGCCGAGAA.

GFP reporter assays and flow-cytometry

GFP reporter assays and flow-cytometry experiments were performed on 24-h incubated cultures as previously described (46). Inducers were added directly to the growth media at the time of inoculation where relevant.

Acknowledgements

The authors would like to thank Christian Rodgers for providing barley seeds for the experiments in this study.

References

1. Awika JM. Major Cereal Grains Production and Use around the World. Advances in Cereal Science: Implications to Food Processing and Health Promotion. ACS Symposium Series. 1089: American Chemical Society; 2011. p. 1-13.

2. Udvardi M, Brodie EL, Riley W, Kaeppler S, Lynch J. Impacts of agricultural nitrogen on the

548 environment and strategies to reduce these impacts. Procedia Environ Sci. 2015;29:303.
549 3. Bonilla Cedrez C, Chamberlin J, Guo Z, Hijmans RJ. Spatial variation in fertilizer prices in Sub-
550 Saharan Africa. PLOS ONE. 2020;15(1):e0227764.
551 4. Holden ST. Fertilizer and sustainable intensification in Sub-Saharan Africa. Glob Food Sec.
552 2018;18:20-6.
553 5. Liu H, Carvalhais LC, Crawford M, Singh E, Dennis PG, Pieterse CMJ, et al. Inner plant values:
554 diversity, colonization and benefits from endophytic bacteria. Front Microbiol. 2017;8:2552.
555 6. Souza Rd, Ambrosini A, Passaglia LMP. Plant growth-promoting bacteria as inoculants in
556 agricultural soils. Genet Mol Biol. 2015;38(4):401-19.
557 7. Knights HE, Jorrin B, Haskett TL, Poole PS. Deciphering bacterial mechanisms of root
558 colonization. Environmental Microbiology Reports. 2021;13(4):428-44.
559 8. Herridge DF, Peoples MB, Boddey RM. Global inputs of biological nitrogen fixation in agricultural
560 systems. Plant Soil. 2008;311(1):1-18.
561 9. Haskett TL, Tkacz A, Poole PS. Engineering rhizobacteria for sustainable agriculture. ISME J.
562 2020;15:949–64.
563 10. Pedrosa FO, Oliveira ALM, Guimarães VF, Etto RM, Souza EM, Furmam FG, et al. The
564 ammonium excreting *Azospirillum brasilense* strain HM053: a new alternative inoculant for maize.
565 Plant Soil. 2020;451(1):45-56.
566 11. Dobbelaere S, Croonenborghs A, Thys A, Ptacek D, Vanderleyden J, Dutto P, et al. Responses of
567 agronomically important crops to inoculation with *Azospirillum*. Funct Plant Biol. 2001;28(9):871-9.
568 12. Díaz-Zorita M, Fernández-Canigia MV. Field performance of a liquid formulation of *Azospirillum*
569 *brasilense* on dryland wheat productivity. Eur J Soil Biol. 2009;45(1):3-11.
570 13. Bueno Batista M, Dixon R. Manipulating nitrogen regulation in diazotrophic bacteria for
571 agronomic benefit. Biochem Soc Trans. 2019;47(2):603-14.
572 14. Inomura K, Bragg J, Follows MJ. A quantitative analysis of the direct and indirect costs of
573 nitrogen fixation: a model based on *Azotobacter vinelandii*. ISME J. 2017;11(1):166-75.
574 15. Bueno Batista M, Brett P, Appia-Ayme C, Wang Y-P, Dixon R. Disrupting hierarchical control of
575 nitrogen fixation enables carbon-dependent regulation of ammonia excretion in soil diazotrophs.

576 PLoS Genet. 2021;17(6):e1009617.

577 16. Colnaghi R, Green A, He L, Rudnick P, Kennedy C. Strategies for increased ammonium
578 production in free-living or plant associated nitrogen fixing bacteria. Plant Soil. 1997;194(1):145-54.

579 17. Bali A, Blanco G, Hill S, Kennedy C. Excretion of ammonium by a *nifL* mutant of *Azotobacter*
580 *vinelandii* fixing nitrogen. Applied Environmental Microbiology. 1992;58(5):1711-8.

581 18. Brewin B, Woodley P, Drummond M. The basis of ammonium release in nifL mutants of
582 *Azotobacter vinelandii*. J Bacteriol. 1999;181(23):7356-62.

583 19. Barney BM, Eberhart LJ, Ohlert JM, Knutson CM, Plunkett MH. Gene deletions resulting in
584 increased nitrogen release by *Azotobacter vinelandii*: application of a novel nitrogen biosensor. Appl
585 Environ Microbiol. 2015;81(13):4316-28.

586 20. Mus F, Khokhani D, MacIntyre AM, Rugoli E, Dixon R, Ané J-M, et al. Genetic determinants of
587 ammonium excretion in *nifL* mutants of *Azotobacter vinelandii*. Appl Environ Microbiol.
588 2022;0(ja):AEM.01876-21.

589 21. Martinez-Argudo I, Little R, Dixon R. Role of the amino-terminal GAF domain of the NifA
590 activator in controlling the response to the antiactivator protein NifL. Mol Microbiol.
591 2004;52(6):1731-44.

592 22. Reyes-Ramirez F, Little R, Dixon R. Mutant forms of the *Azotobacter vinelandii* transcriptional
593 activator NifA resistant to inhibition by the NifL regulatory protein. J Bacteriol. 2002;184(24):6777.

594 23. Ghenov F, Gerhardt ECM, Huergo LF, Pedrosa FO, Wassem R, Souza EM. Characterization of
595 glutamine synthetase from the ammonium-excreting strain HM053 of *Azospirillum brasilense*. Braz J
596 Biol. 2021;82:e235927.

597 24. Machado HB, Funayama S, Rigo LU, Pedrosa FO. Excretion of ammonium by *Azospirillum*
598 *brasilense* mutants resistant to ethylenediamine. Can J Microbiol. 1991;37(7):549-53.

599 25. Michel-Reydellet N, Desnoues N, Elmerich C, Kaminski PA. Characterization of *Azorhizobium*
600 *caulinodans glnB* and *glnA* genes: involvement of the P_{II} protein in symbiotic nitrogen fixation. J
601 Bacteriol. 1997;179(11):3580-7.

602 26. Toukdarian A, Saunders G, Selman-Sosa G, Santero E, Woodley P, Kennedy C. Molecular
603 analysis of the *Azotobacter vinelandii glnA* gene encoding glutamine synthetase. J Bacteriol.

1990;172(11):6529-39.

27. Ambrosio R, Ortiz-Marquez JCF, Curatti L. Metabolic engineering of a diazotrophic bacterium improves ammonium release and biofertilization of plants and microalgae. Metab Eng. 2017;40:59-68.

28. Michel-Reydellet N, Kaminski PA. *Azorhizobium caulinodans* P_{II} and GlnK proteins control nitrogen fixation and ammonia assimilation. J Bacteriol. 1999;181(8):2655-8.

29. Schnabel T, Sattely E. Engineering posttranslational regulation of glutamine synthetase for controllable ammonia production in the plant symbiont *Azospirillum brasilense*. Applied Environmental Microbiology. 2021;87(14):e0058221.

30. Stadtman ER. Regulation of glutamine synthetase activity. EcoSal Plus. 2004;1(1).

31. Jaggi R, van Heeswijk WC, Westerhoff HV, Ollis DL, Vasudevan SG. The two opposing activities of adenylyl transferase reside in distinct homologous domains, with intramolecular signal transduction. EMBO J. 1997;16(18):5562-71.

32. Huergo LF, Chandra G, Merrick M. PII signal transduction proteins: nitrogen regulation and beyond. FEMS Microbiol Rev. 2013;37(2):251-83.

33. Kennedy C, Doetsch N, Meletzus D, Patriarca E, Amar M, Iaccarino M. Ammonium sensing in nitrogen fixing bacteria: Functions of the *glnB* and *glnD* gene products. Plant Soil. 1994;161(1):43-57.

34. Liang YY, de Zamaroczy M, Arséne F, Paquelin A, Elmerich C. Regulation of nitrogen fixation in *Azospirillum brasilense* Sp7: Involvement of *nifA*, *glnA* and *glnB* gene products. FEMS Microbiol Lett. 1992;100(1-3):113-9.

35. de Zamaroczy M. Structural homologues P(II) and P(Z) of *Azospirillum brasilense* provide intracellular signalling for selective regulation of various nitrogen-dependent functions. Mol Microbiol. 1998;29(2):449-63.

36. Meletzus D, Rudnick P, Doetsch N, Green A, Kennedy C. Characterization of the *glnK-amtB* operon of *Azotobacter vinelandii*. J Bacteriol. 1998;180(12):3260-4.

37. Hanson TE, Forchhammer K, de Marsac NT, Meeks JC. Characterization of the *glnB* gene product of *Nostoc punctiforme* strain ATCC 29133: *glnB* or the PII protein may be essential. Microbiology.

1998;144(6):1537-47.

38. Jonsson A, Nordlund S, Teixeira PF. Reduced activity of glutamine synthetase in *Rhodospirillum rubrum* mutants lacking the adenylyltransferase GlnE. Res Microbiol. 2009;160(8):581-4.

39. Mus F, Tseng A, Dixon R, Peters JW, Pettinari MJ. Diazotrophic growth allows *Azotobacter vinelandii* to overcome the deleterious effects of a *glnE* deletion. Appl Environ Microbiol. 2017;83(13):e00808-17.

40. Foor F, Janssen KA, Magasanik B. Regulation of synthesis of glutamine synthetase by adenylylated glutamine synthetase. Proc Natl Acad Sci. 1975;72(12):4844-8.

41. Parish T, Stoker NG. *glnE* is an essential gene in *Mycobacterium tuberculosis*. J Bacteriol. 2000;182(20):5715-20.

42. Carroll P, Pashley CA, Parish T. Functional analysis of GlnE, an essential adenylyl transferase in *Mycobacterium tuberculosis*. J Bacteriol. 2008;190(14):4894-902.

43. Schnabel T, Sattely E. Improved stability of engineered ammonia production in the plant-symbiont *Azospirillum brasilense*. ACS Synth Biol. 2021;10(11):2982-96.

44. Ryu MH, Zhang J, Toth T, Khokhani D, Geddes BA, Mus F, et al. Control of nitrogen fixation in bacteria that associate with cereals. Nat Microbiol. 2020;5(2):314-30.

45. Geddes BA, Ryu MH, Mus F, Garcia Costas A, Peters JW, Voigt CA, et al. Use of plant colonizing bacteria as chassis for transfer of N_2-fixation to cereals. Curr Opin Biotechnol. 2015;32:216-22.

46. Haskett TL, Paramasivan P, Mendes MD, Green P, Geddes B, Knights HE, et al. Engineered plant control of associative nitrogen fixation. Proc Natl Acad Sci. 2022;*in press*.

47. Geddes BA, Paramasivan P, Joffrin A, Thompson AL, Christensen K, Jorrin B, et al. Engineering transkingdom signalling in plants to control gene expression in rhizosphere bacteria. Nat Commun. 2019;10(1):3430.

48. Bender RA, Janssen KA, Resnick AD, Blumenberg M, Foor F, Magasanik B. Biochemical parameters of glutamine synthetase from *Klebsiella aerogenes*. J Bacteriol. 1977;129(2):1001-9.

49. Bolleter WT, Bushman CJ, Tidwell PW. Spectrophotometric Determination of Ammonia as Indophenol. Analytical Chemistry. 1961;33(4):592-4.

50. Schulte CCM, Borah K, Wheatley RM, Terpolilli JJ, Saalbach G, Crang N, et al. Metabolic

660 control of nitrogen fixation in rhizobium-legume symbioses. Science Advances. 2021;7(31).
661 51. Rutten PJ, Steel H, Hood GA, Ramachandran VK, McMurtry L, Geddes B, et al. Multiple sensors
662 provide spatiotemporal oxygen regulation of gene expression in a Rhizobium-legume symbiosis.
663 PLoS Genet. 2021;17(2):e1009099.
664 52. Fischer H-M, Hennecke H. Direct response of *Bradyrhizobium japonicum nifA*-mediated nif gene
665 regulation to cellular oxygen status. Mol Gen Genet. 1987;209(3):621-6.
666 53. Michel-Reydellet N, Desnoues N, de Zamaroczy M, Elmerich C, Kaminski PA. Characterisation
667 of the *glnK-amtB* operon and the involvement of AmtB in methylammonium uptake in *Azorhizobium*
668 *caulinodans*. Mol Gen Genet. 1998;258(6):671-7.
669 54. Drepper T, Gross S, Yakunin AF, Hallenbeck PC, Masepohl B, Klipp W. Role of GlnB and GlnK
670 in ammonium control of both nitrogenase systems in the phototrophic bacterium *Rhodobacter*
671 *capsulatus*. Microbiology. 2003;149(Pt 8):2203-12.
672 55. Pekgöz G, Gündüz U, Eroğlu I, Yücel M, Kovács K, Rákhely G. Effect of inactivation of genes
673 involved in ammonium regulation on the biohydrogen production of *Rhodobacter capsulatus*.
674 International Journal of Hydrogen Energy. 2011;36(21):13536-46.
675 56. Neilson AH, Nordlund S. Regulation of nitrogenase synthesis in intact cells of *Rhodospirillum*
676 *rubrum*: inactivation of nitrogen fixation by ammonia, L-glutamine and L-asparagine. J Gen
677 Microbiol. 1975;91(1):53-62.
678 57. Turpin DH, Edie SA, Canvin DT. In vivo nitrogenase regulation by ammonium and methylamine
679 and the effect of MSX on ammonium transport in *Anabaena* flos-aquae. Plant Physiol.
680 1984;74(3):701-4.
681 58. Reich S, Almon H, Böger P. Short-term effect of ammonia on nitrogenase activity of Anabaena
682 variabilis (ATCC29413). FEMS Microbiol Lett. 1986;34(1):53-6.
683 59. Jones BL, Monty KJ. Glutamine as a feedback inhibitor of the *Rhodopseudomonas sphaeroides*
684 nitrogenase system. J Bacteriol. 1979;139(3):1007-13.
685 60. Kuczius T, Kleiner D. Ammonia-excreting mutants of *Klebsiella pneumoniae* with a pleiotropic
686 defect in nitrogen metabolism. Arch Microbiol. 1996;166(6):388-93.
687 61. Masepohl B, Drepper T, Paschen A, Gross S, Pawlowski A, Raabe K, et al. Regulation of nitrogen

688 fixation in the phototrophic purple bacterium *Rhodobacter capsulatus*. J Mol Microbiol Biotechnol.
689 2002;4(3):243-8.
690 62. Masepohl B, Klipp W. Organization and regulation of genes encoding the molybdenum
691 nitrogenase and the alternative nitrogenase in *Rhodobacter capsulatus*. Arch Microbiol.
692 1996;165(2):80-90.
693 63. Wang D, Xu A, Elmerich C, Ma LZ. Biofilm formation enables free-living nitrogen-fixing
694 rhizobacteria to fix nitrogen under aerobic conditions. ISME J. 2017;11(7):1602-13.
695 64. Bozsoki Z, Gysel K, Hansen SB, Lironi D, Krönauer C, Feng F, et al. Ligand-recognizing motifs
696 in plant LysM receptors are major determinants of specificity. Science. 2020;369(6504):663-70.
697 65. Beringer JE. R factor transfer in *Rhizobium leguminosarum*. Microbiology. 1974;84(1):188-98.
698 66. Poole PS, Schofield NA, Reid CJ, Drew EM, Walshaw DL. Identification of chromosomal genes
699 located downstream of *dctD* that affect the requirement for calcium and the lipopolysaccharide layer
700 of *Rhizobium leguminosarum*. Microbiology. 1994;140 (Pt 10):2797-809.
701 67. Brown CM, Dilworth MJ. Ammonia assimilation by *Rhizobium* cultures and bacteroids.
702 Microbiology. 1975;86(1):39-48.
703 68. Geddes BA, Mendoza-Suárez MA, Poole PS. A bacterial expression vector archive (BEVA) for
704 flexible modular assembly of golden gate-compatible vectors. Front Microbiol. 2019;9:3345.
705 69. Weber E, Engler C, Gruetzner R, Werner S, Marillonnet S. A modular cloning system for
706 standardized assembly of multigene constructs. PLoS One. 2011;6(2):e16765.
707 70. Thoma S, Schobert M. An improved *Escherichia coli* donor strain for diparental mating. FEMS
708 Microbiol Lett. 2009;294(2):127-32.
709 71. Choi KH, Schweizer HP. mini-Tn7 insertion in bacteria with single attTn7 sites: example
710 *Pseudomonas aeruginosa*. Nat Protoc. 2006;1(1):153-61.
711 72. Sprouffske K, Wagner A. Growthcurver: an R package for obtaining interpretable metrics from
712 microbial growth curves. BMC Bioinformatics. 2016;17(1):172.
713 73. Donald RG, Ludwig RA. *Rhizobium* sp. strain ORS571 ammonium assimilation and nitrogen
714 fixation. J Bacteriol. 1984;158(3):1144-51.
715 74. Haskett TL, Knights HE, Jorrin B, Mendes MD, Poole PS. A simple in situ assay to assess plant-

716 associative bacterial nitrogenase activity. Front Microbiol. 2021;12(1598).

717 75. Ling J, Wang H, Wu P, Li T, Tang Y, Naseer N, et al. Plant nodulation inducers enhance horizontal
718 gene transfer of *Azorhizobium caulinodans* symbiosis island. Proc Natl Acad Sci.
719 2016;113(48):13875-80.

720 Supporting Information Captions

721 **S1 Fig. Characterisation of synthetic ribosome binding sites in *Ac*LP.** Each RBS was fused to GFP
722 under expression by the strong synthetic promoter J23104 on plasmid pOGG024 and GFP was
723 measured after 24-h incubation in UMS media (n = 3). Relative luminescence units are defined here
724 as GFP fluorescence / OD600λnm. The RBS nucleotide sequences are provided in S1 File.

725

726 **S2 Fig. Expression and total activity of glutamine synthetase (*glnA*, GS) is elevated in *Ac*RGl. (a)**
727 Total specific activity of both adenylated (inactive) and unadenylated (active) forms of GS was
728 measured in whole cells grown for 24-h as determined by γ-glutamyl transferase assays (n = 5). **(b)**
729 *glnA* expression was quantified relative to the housekeeping gene *recA* by RT-qPCR in cells growth
730 for 3-h. All cultures for assays were grown in N_2-fixing conditions (N-free UMS media with 3% O_2 in
731 the headspace). Error bars represent one SEM. Independent two-tailed students t-tests were used to
732 compare means. ***P < 0.001.

733

734 **S3 Fig. Induction of the *Sinorhizobium meliloti* 1021 naringenin-inducible *PnodA* promoter in**
735 ***Ac*LP (a)** Genetic schematic (not to scale) of the low-copy (RK2 replicon) naringenin-inducible *GFP*
736 reporter plasmid pOPS1536. **(b)** GFP induction in *Ac*LP (n = 3) harbouring pOPSXXX in response to
737 naringenin supplemented *in vitro*. Relative luminescence units are defined here as GFP fluorescence /
738 OD600λnm.

739

740 **S4 Fig. Total activity of glutamine synthetase (GS) in Δ*glnE* mutants expressing unidirectional**
741 **adenylyl transferases from the non-induced P*nodA* promoter (a)** Total specific activity of both
742 adenylated (inactive) and unadenylated (active) forms of GS was measured in whole cells grown in

N_2-fixing conditions (N-free UMS media with 3% O_2 in the headspace) for 3-h as determined by γ-glutamyl transferase assays (n = 5 for wild-type *Ac*LP or n = 3 for other strains). Error bars represent one SEM. Independent two-tailed students t-tests were used to compare means against the wild-type (WT) *Ac*LP as a reference. Not significant (ns) indicates P > 0.05, *P < 0.05.

S5 Fig. NH_3 excretion is sub-optimal in Δ*glnE* mutants expressing unidirectional adenylyl transferases from the P*nodA* promoter induced with naringenin. Spectrophotometric determination of NH_3 in media of cultures induced with 5 μM naringenin grown for 24-h in N_2-fixing conditions (N-free UMS media with 3% O_2 in the headspace). Error bars represent one SEM. n = 3 for wild-type *Ac*LP Δ*glnE* or n = 6 for other strains.

S6 Fig. Growth statistics for control strains and Δ*glnE* mutants expressing unidirectional adenylyltransferases. Mean generation times and the max OD600λnm (i.e. the carrying capacity, k) were calculated from standard curves of cultures grown in UMS media at 21% O_2. Representative growth curves are provided in Fig 3c and Fig 5b. Strains highlighted in white are wild-type (WT) *Ac*LP and *Ac*LPΔ*glnE* controls, strains highlighted in pink are *Ac*LPΔ*glnE* carrying P*nodA* [RBS] uAT-DT16 modules on parent plasmid pOGG093 and strains highlighted in blue are *Ac*LPΔ*glnE* carrying mini-Tn*7* integrated P*nifH* [RBS] uAT-*Ac2*-DT16 modules.

S7 Fig. Rhizopine control of N_2 fixation alone does not permit NH_3 excretion. Spectrophotometric determination of NH_3 in media of n = 3 cultures grown for 24-h in N_2-fixing conditions. Error bars represent one SEM. Strain *Azospirillum brasilense* HM053 was used here as a positive control.

S8 Fig. $NifA_{L94Q/D95Q}$ activity is tolerant to ambient environmental oxygen. (a) Genetic schematic (not to scale) of the rhizopine *nifA*$_{L94Q/D95Q}$-*rpoN* controller plasmid with P*nifH*::*GFP* reporter fusion pSIN03. **(b)** P*nifH* promoter activity was measured in n = 4 cultures grown for 24-h under the conditions indicated. Relative fluorescence units (RFU) are defined here as GFP fluorescence /

OD600λnm. Error bars represent one SEM. Independent two-tailed students t-tests with Bonferroni-holm adjustment were used to compare means. $P > 0.05$. $^{**}P < 0.01$, $^{***}P < 0.001$.

S1 Table. Flowcytometry statistics for rhizopine-inducible GFP expression in *Ac*LP carrying pOPS1052

S2 Table. Plasmids used in this study